1   **Title: SARS-CoV-2 Viral Clearance and Evolution Varies by Extent of**

2   **Immunodeficiency**

3   **Authors**: Yijia Li*[1 2 3] , Manish C. Choudhary*[1] , James Regan*[1] , Julie Boucau[4] , Anusha

4   Nathan[4 5] , Tessa Speidel[6] , May Yee Liew[2 7] , Gregory E. Edelstein[1] , Yumeko Kawano[1] ,

5   Rockib Uddin[2 7] , Rinki Deo[1] , Caitlin Marino[4] , Matthew A. Getz[4] , Zahra Reynold[2] , Mamadou

6   Barry[2] , Rebecca F. Gilbert[2] , Dessie Tien[2] , Shruti Sagar[2] , Tammy D. Vyas[2] , James P. Flynn[1] ,

7   Sarah P. Hammond[2] , Lewis A. Novack[1], Bina Choi[1], Manuela Cernadas[1], Zachary S. Wallace[2] ,

8   Jeffrey A. Sparks[1] , Jatin M. Vyas[2 4] , Michael S. Seaman[6] , Gaurav D. Gaiha[2 4] , Mark J.

9   Siedner[#2] , Amy K. Barczak[#2 4] , Jacob E. Lemieux[#2 7] , Jonathan Z. Li[#1]

10

11   **Affiliations**:

12   1. Department of Medicine, Brigham and Women's Hospital, Harvard Medical School, Boston, MA, USA

13   2. Department of Medicine, Massachusetts General Hospital, Harvard Medical School, Boston, MA, USA

14   3. University of Pittsburgh Medical Center, Pittsburgh, PA, USA

15   4. Ragon Institute of MGH, MIT and Harvard, Cambridge, MA, USA

16   5. Program in Health Sciences and Technology, Harvard Medical School and Massachusetts Institute of

17   Technology, Boston, MA 02115, USA

18   6. Center for Virology and Vaccine Research, Beth Israel Deaconess Medical Center, Harvard Medical

19   School, Boston, MA, USA

20   7. Broad Institute of MIT and Harvard, Cambridge, MA, USA

21

22   *, # Equal contribution

23

24

Abstract

26   Despite vaccination and antiviral therapies, immunocompromised individuals are at risk for

27   prolonged SARS-CoV-2 infection, but the immune defects that predispose to persistent COVID-

28   19 remain incompletely understood. In this study, we performed detailed viro-immunologic

29   analyses of a prospective cohort of participants with COVID-19. The median time to nasal viral

30   RNA and culture clearance in the severe hematologic malignancy/transplant group (S-HT) were

31   72 and 40 days, respectively, which were significantly longer than clearance rates in the severe

32   autoimmune/B-cell deficient (S-A), non-severe, and non-immunocompromised groups

33   (P<0.001). Participants who were severely immunocompromised had greater SARS-CoV-2

34   evolution and a higher risk of developing antiviral treatment resistance. Both S-HT and S-A

35   participants had diminished SARS-CoV-2-specific humoral, while only the S-HT group had

36   reduced T cell-mediated responses. This highlights the varied risk of persistent COVID-19

37   across immunosuppressive conditions and suggests that suppression of both B and T cell

38   responses results in the highest contributing risk of persistent infection.

39 **Main Text**

40 **Introduction**

41 Coronavirus Disease 2019 (COVID-19) vaccinations have drastically transformed the landscape

42 of the COVID-19 pandemic by offering significant protection against infection acquisition, and

43 severe diseases(*1, 2*), and ultimately have averted tens of millions of deaths(*3*). Unfortunately,

44 not all individuals respond to vaccination equally well, and immunocompromised individuals can

45 have poor vaccine responses(*4, 5*) and worse COVID-19-related outcomes(*6, 7*). Each new

46 variant of Severe Acute Respiratory Syndrome Coronavirus-2 (SARS-CoV-2) brings risks of

47 resistance to current treatments, particularly targeted antibody therapies(*8, 9*), resistance to

48 vaccine-induced and naturally acquired immunity(*9, 10*), and increased transmissibility(*10*).

49 Immunocompromised individuals have been observed to harbor detectable SARS-CoV-2 virus

50 for longer than non-immunocompromised individuals(*11-13*). Such individuals represent a

51 potential origin of novel SARS-CoV-2 variants as persistent infection has been associated with

52 accelerated viral evolution(*11, 13*). However, the immunocompromised state is composed of a

53 range of conditions and immune defects. These defects that predispose to persistent COVID-

54 19 remain under-characterized. While there have been a number of case reports of persistent

55 COVID-19 in immunosuppressed individuals(*11-16*) showing excessively prolonged viral

56 shedding, persistent disease, and intra-host virological genetic diversity, there remains a need

57 for larger scale studies with a comprehensive virologic and immunologic characterization to

58 better elucidate the immunologic risk factors for and mechanisms of persistent infection. To this

59 end, we hereby present a detailed longitudinal virological and immunological analysis of a

60 cohort of immunocompromised and non-immunocompromised participants with SARS-CoV-2

61 infection with the goal of characterizing the virologic spectrum of persistent infection and

62 exploring the immunologic determinants that predispose to its occurrence.

63 **Results**

64 **Participant Characteristics**

65 Fifty-six immunocompromised participants and 184 non-immunocompromised participants

66 enrolled in the POSITIVES longitudinal cohort study were included in this analysis (*17-19*).

67 Demographic information and key viral characteristics are shown in Table 1.

68 Immunocompromised participants were significantly older than non-immunocompromised

69 controls (median 55 vs 46 years, P=0.001), and more likely to receive monoclonal antibody

70 (mAb) and/or antiviral treatment against SARS-CoV-2. The two groups had comparable sex,

71 race, and ethnicity profiles and a similar median time from symptom onset/first positive COVID-

72 19 test to enrollment (5 vs 4 days). We further subdivided immunocompromised participants into

73 the severe hematologic-oncology/transplant (S-HT, n=12), severe autoimmune/B-cell deficient

74 (S-A, n=13) and non-severe (NS, n=31) groups (refer to Supplementary Tables 1 and 2 for

75 detailed categorization). Three participants died due to severe COVID-19 or COVID-19 related

76 complications, all of whom were in the immunocompromised sub-group (S-HT and S-A).

77

78 **Delayed Viral Clearance in Hematologic Oncology and Transplant Participants**

79 We first aimed to characterize viral dynamics in the upper respiratory tract in participants with

80 different categories of immunocompromising conditions. Immunocompromised and non-

81 immunocompromised participants had similar peak vRNA levels (5.1, 5.1, 4.9, and 5.7 $\log_{10}$

82 SARS-CoV-2 copies/ml in S-HT, S-A, NS and non-immunocompromised groups, P=0.5).

83 However, the rates of nasal vRNA decay were significantly different between the

84 immunocompromising categories, with the S-HT group demonstrating significantly slower viral

85 clearance compared to other groups (Fig. 1a and 1b). Median time to nasal vRNA clearance in

86 the S-HT group was 72 days (95% confidence interval [CI] 5, not available [NA]) compared to 7

87 (6, NA) days for the S-A, 11 (8, 16) days for the NS and 11 (10, 12) days for the non-

88 immunocompromised group (Fig. 1b, Log-rank P=0.002). Similarly, the S-HT group experienced

89   a significant delay in the clearance of culturable virus (Fig. 1c and 1d). Median time to viral

90   culture clearance in the S-HT group was 40 days (95%CI 5, NA) compared to 6.5 (5, NA) days

91   for the S-A group, 6 days (5, 7) for the NS group and 7 days (6, 7) for the non-

92   immunocompromised group (Fig. 1d, log-rank P<0.001, Fig. 1d). After 30 days from symptom

93   onset or first positive test, 50%, 15%, and 6.5% of participants from S-HT, S-A and NS groups

94   had detectable vRNA, compared to 0% in non-immunocompromised group (P<0.0001,

95   Supplementary Fig. 1a). In addition, 50% of S-HT and 8.3% of S-A participants still had

96   culturable virus, compared to 0% in the NS and non-immunocompromised groups after 30 days

97   (P<0.0001, Supplementary Fig. 1b). Compared to the non-immunocompromised group, the S-

98   HT group was significantly associated with delayed vRNA clearance (adjusted hazard ratio

99   [aHR] for viral clearance, 0.32, 95%CI 0.12-0.83, P=0.02) and culturable virus clearance (aHR

100   0. 27 for viral clearance, 95% CI 0.12-0.63, P=0.002), after adjusting for demographics, number

101   of vaccinations and antiviral use (Table 2).

102

103   **Increased Viral Evolution and Genetic Diversity in Immunocompromised Participants**

104   We used gene-specific next-generation sequencing approach to quantify the number of unique

105   intra-host single-nucleotide variants (iSNVs) in the S gene present at >3% frequency within

106   each sample. This analysis was limited to participants with a viral genome available both at

107   baseline and at least one follow-up timepoint. Severely immunocompromised (S-HT and S-A)

108   participants harbored a greater number of iSNVs over time compared to NS and non-

109   immunocompromised group participants, although these comparisons did not reach statistic

110   significance (Fig. 2a). To evaluate viral diversity, we calculated the average pairwise distance

111   both at the nucleotide and at the amino-acid level. Nucleotide average pairwise distance was

112   significantly higher in the severe immunocompromised (S-HT and S-A) group compared to

113   either non-severe (4.0E-4 vs 8.2E-5, P<0.001 Dunn's test with Benjamini-Hochberg adjustment)

114   or non-immunocompromised groups (4.0E-4 vs 2.3E-5, P<0.001, Fig. 2b). Similar results were

115   obtained when the average pairwise distances were calculated for amino acids (Supplementary

116   Fig. 2a). Among participants with longitudinal sequences, 39% of the participants in

117   immunocompromised group versus 12% in the non-immunocompromised group had evidence

118   of viral nucleotide changes (Fisher's exact P<0.001, Fig. 2c). These nucleotide changes were

119   distributed across the entire length of the S gene (Fig. 2d).

120

121   **Increased Risk of Treatment-Emergent Resistance to Anti-SARS-CoV-2 Monoclonal**

122   **Antibody Therapy**

123   Deep sequencing analysis of Spike gene was carried out to evaluate the dynamics of mutation

124   emergence in the presence of mAb treatment as earlier reports have shown evidence of mAb

125   resistance emergence both in immunocompromised and non-immunocompromised

126   participants(*13, 20-29*). In total, 34 participants across different study groups received mAb

127   therapy, 10 in S-HT, 9 in S-A, 5 in NS, and 10 in non-immunocompromised groups (Details in

128   Supplementary Table 3). Of these, we were able to evaluate the risk of resistance emergence in

129   a subset of participants for whom sequences were available at both baseline and at least one

130   follow-up time point. Five out of nine (56%) severely immunocompromised participants (S-HT

131   and S-A) developed mAb-specific resistance mutations (Supplementary Fig. 2b). This was a

132   significantly higher rate than that found in the non-severe or non-immunocompromised groups

133   (0/11 [0%] combined, Fisher's exact P=0.008) (Fig 2e).

134

135   **Suboptimal Humoral Response in Severely Immunocompromised Participants**

136   We next characterized the antibody response in immunocompromised and non-

137   immunocompromised participants. In participants whose serum sample was available (n=94),

138   including those who had previously received monoclonal antibodies, we found no significant

139   difference in nAb titers between the different immunocompromised and non-

140   immunocompromised groups at early and later sampling time points, although this analysis may

141   have been limited due to individuals who received anti-SARS-CoV-2 monoclonal antibody

142   infusion before sample collection (either therapeutic or pre-exposure prophylaxis) (Fig. 3a and

143   3b). The non-immunocompromised group had a significant increase in anti-ancestral and anti-

144   variant spike nAb levels during follow-up, whereas we did not observe a significant increase in

145   antibody levels in the immunocompromised group (Fig. 3a and 3b). However, after excluding

146   individuals with exposure to mAb therapies, the severe immunocompromised group showed no

147   significant changes in either anti-ancestral or anti-variant Spike nAb levels, while the non-severe

148   immunocompromised group demonstrated a moderate increase and the non-

149   immunocompromised group demonstrated the greatest increase in nAb levels, plateauing at day

150   25-30 (Fig. 3c and d).

151

152   In a generalized estimating equation (GEE) model adjusted for factors associated with nAb

153   levels, severely immunocompromised participants were only able to mount 0.18-fold

154   (approximately 5-fold lower) of the anti-ancestral Spike antibody (95% CI 0.05-0.60) and 0.08-

155   fold (approximately 12-fold lower) of the anti-variant Spike antibody (95% CI 0.03-0.22)

156   compared to non-immunocompromised participants (Supplementary Fig. 3a, b). Non-severe

157   immunocompromised status was not associated with significant differences in nAb changes

158   from acute to post-infection, compared to non-immunocompromised group. In the whole cohort,

159   each dose of vaccinations prior to SARS-CoV-2 infection was associated with 1.70-fold (95% CI

160   1.25 to 2.30) and 1.35-fold (95% CI 1.01 to 1.79) increase in anti-ancestral and anti-variant

161   Spike antibody levels, respectively (Supplementary Fig. 3ab).

162

163   We also evaluated binding antibody against nucleocapsid protein because this assay is not

164   affected by monoclonal antibody use. Similar to nAb, individuals in the S-HT and S-A sub-

165   groups had significantly blunted increases in nucleocapsid binding Ab development from acute

166   to post-infection, and significantly lower binding Ab levels compared to NS and non-

167   immunocompromised groups (Fig. 3e). Longitudinally, binding Ab levels in NS and non-

168   immunocompromised groups plateaued around day 20-25 at a level of 1-1.5 $\log_{10}$ IU/ml, while

169   S-HT/S-A groups exhibited delayed development to a level below 1 $\log_{10}$ IU/ml after day 50 (Fig.

170   3f).

171

172   **T Cell Responses**

173   In a recent study, Apostolidis et al. demonstrated elevated spike-specific CD8^{+} T cell responses

174   in COVID-19 mRNA vaccinated participants with multiple sclerosis receiving anti-CD20

175   treatment compared to healthy controls(*30*). However, it remains largely unknown if different

176   types and levels of immunosuppression are associated with a similar T cell immunophenotype.

177   To this end, we profiled the T cell effector function using enzyme-linked immunosorbent spot

178   (ELISpot) and antigen-specific proliferation assay for a selected group of participants based on

179   sample availability. The non-immunocompromised group had lower interferon gamma (IFN-γ)

180   producing units per million cells upon stimulation at both blood draws (acute infection 0-14 days,

181   and post-acute 15-60 days after symptom onset or first positive COVID-19 test) compared to

182   both NS and S-A groups in response to both ancestral and variant-specific Spike peptide pools

183   (Fig. 4a). Individuals in the S-A group tended to have the highest levels of CD4+ and CD8^{+} T

184   cell proliferation upon spike peptide pool stimulation, especially compared to the S-HT and non-

185   immunocompromised individuals (Fig. 4bc and Supplementary Fig. 4). In longitudinal analysis,

186   the S-HT group showed poor functional CD4^{+} and CD8^{+} T cell proliferation, despite a

187   comparable IFN-γ secretion level compared to the non-immunocompromised group (Fig. 4d). In

188   contrast, the S-A group showed robust T cell proliferation over time, in response to both

189   ancestral and variant-specific spike peptide pools compared to all other groups, suggestive of

190   either an antigen-stimulated compensatory effect in the setting of B cell deficiency or a

191   medication-related T cell priming.

Discussion

Understanding viral and immune control characteristics of COVID-19 infection is crucial to our

ability to care for immunocompromised individuals at greatest risk of persistent and severe

infection. Moreover, it can guide public health interventions and shed light on vaccine

development that protects immunocompromised individuals. In this study, we performed an in-

depth virologic and immunologic evaluation of a cohort of immunocompromised and non-

immunocompromised individuals. We demonstrated a hierarchy of immunocompromised

conditions that increase the risk of delayed viral clearance and SARS-CoV-2 evolution.

Furthermore, we identified the varied risk of persistent COVID-19 across immunosuppressive

conditions and suppression of both B and T cell responses in those at the highest risk of

persistent infection. Specifically, we found that individuals with a history of hematological

malignancy and organ transplant demonstrated the greatest delay in viral clearance that may be

mediated by suppression of both the B and T cell responses. In contrast, those with B cell

immunodeficiency had an intermediate risk of chronic infection in the setting of an immune

response showing compensatory heightened levels of SARS-CoV-2-specific T cell function.

Our cohort study confirmed findings from prior case reports and case series. In a review by

Dioverti et al., the authors summarized cases of persistent COVID-19 lasting from

approximately one month to one year(*31*). These included a spectrum of immunocompromised

hosts from individuals with solid organ transplants, hematological malignancy(*14, 20, 22, 23, 25,*

29, 32-36), and autoimmune diseases receiving immunosuppressive therapies. However,

immunocompromise is a broad spectrum and, until now it has not been clear which

immunosuppressive conditions represent the greatest risk for persistent infection. The results of

our study provide critical insight as to the hierarchy of risk for delayed SARS-CoV-2 RNA and

culture clearance, and viral evolution. Specifically, we found that demonstrated that individuals

with solid organ transplant and hematological malignancy are associated with the longest period

218   of viral RNA and culturable viral shedding, followed by severely immunocompromised

219   participants with autoimmune conditions receiving B-cell depleted therapy and/or those with B

220   cell deficiency. Participants with mild non-severe immunocompromise, such as those with

221   autoimmune diseases receiving anti-tumor necrosis factor (TNF) treatment, had similar viral

222   shedding dynamics to non-immunocompromised participants.

223

224   There have been several prior case reports of immunosuppressed individuals with chronic

225   COVID-19 and accumulation of viral polymorphisms and drug resistance mutations(*13, 14, 21,*

226   *27, 34*), but there has been little in the way of more systematic evaluation of viral evolution. In

227   this study, we used S gene-specific deep sequencing to assess longitudinal viral evolution and

228   diversity. Our results show that severe immunosuppression is associated with increased viral

229   evolution and diversification. In addition, severe immunocompromised hosts had a greater risk

230   of developing treatment-emergent resistance mutations to mAb therapy when compared to non-

231   immunocompromised group participants. These findings highlight the potential for

232   immunocompromised individuals to serve as a source for SARS-CoV-2 evolution and drug

233   resistance, consistent with isolated reports of immunocompromised hosts implicated in the

234   emergence of highly mutated SARS-CoV-2 variants(*13, 15, 16, 24, 28, 37-40*). It should be

235   noted though that even within the category of severe immunocompromise, participants

236   demonstrated a range of viral diversification and evolution patterns, and additional studies are

237   needed to fully assess the drivers of accelerated viral evolution.

238

239   Another highlight of our study is our use of in-depth analysis of B and T cell responses,

240   including SARS-CoV-2-specific neutralizing and binding antibody levels, as well as ELISpot and

241   T cell proliferation studies. We noted lower levels of neutralizing antibody against both ancestral

242   virus and variant virus in the severe immunocompromised group (less than 10-20% compared

243   to non-immunocompromised individuals), after adjusting for vaccination doses, monoclonal

244   antibody use, and demographic confounders. Each additional dose of vaccination is associated

245   with an approximately 1.5-fold increase in antibody levels in the whole cohort, underscoring the

246   importance of adherence to COVID-19 vaccination recommendations. However, there is

247   evidence that non-B-cell immunity may be sufficient for the clearance of SARS-CoV-2. Early in

248   the pandemic, cases were reported of individuals with X-linked agammaglobulinemia who

249   developed COVID-19 pneumonia, but subsequently recovered despite a lack of SARS-CoV-2-

250   specific immunoglobulins(*41*). In our study, the risk of chronic infection was highest in S-HT

251   participants. This group of participants was found to have both suboptimal humoral and cell-

252   mediated immune responses. The "near-normal" level of effector ELISpot responses in S-HT

253   individuals, compared to the non-immunocompromised group, is the likely the result of exposure

254   to high levels of SARS-CoV-2 antigen, while the reduced proliferation demonstrates

255   compromised functionality. In contrast, the S-A participants had an even more robust SARS-

256   CoV-2-specific proliferative T-cell responses than the non-immunocompromised group,

257   indicating increased levels of functional SARS-CoV-2-specific CD8+ T cell responses, which

258   was associated with an intermediate risk of chronic infection. These results align with some

259   intriguing reports that individuals receiving anti-CD20 treatment may demonstrate a stronger T-

260   cell responses, in particular more robust activation-induced marker-positive CD8+ T cell

261   responses(*30*). We found that both CD8+ T cell response and CD4+ T-cell responses, including

262   proliferation in response to both ancestral and variant-specific spike peptides, were more

263   pronounced in S-A group compared to other non-immunocompromised groups. Together with

264   the results from Apostolidis et al.(*30*), our results raise the question of whether individuals with B

265   cell deficiencies may have a lower risk of persistent SARS-CoV-2 infection due to preserved T

266   cell function, either as a compensatory mechanism or T cell priming by certain B cell-depleting

267   therapies.

268

269   There are several limitations to this study. We included a relatively small number of individuals

270   with malignant hematological conditions or transplant history, and we were able to obtain blood

271   samples from only a subset of the participants to characterize their humoral and T-cell immunity.

272   Larger studies are needed to provide greater precision as to extent of immune defect or

273   immunosuppressive medication that may place patients at the greatest risk of chronic infection

274   and viral evolution. We also did not analyze markers reflecting innate immunity, including

275   soluble inflammatory markers and monocyte phenotypes. Our study focused on virologic and

276   immunologic responses after COVID-19 and it is unclear how these may contribute to

277   persistence and severity of symptoms. Furthermore, we only evaluated Spike-specific humoral

278   and cellular immunity, while immunity targeting other structural or non-structural proteins has

279   been shown to alter disease course(*42, 43*).

280

281   In conclusion, in this prospective cohort of well-characterized individuals with acute COVID-19,

282   we demonstrated a correlation between a hierarchy of immunocompromised conditions and

283   SARS-CoV-2 viral shedding, viral evolution, and adaptive immunity. Our results highlight the

284   finding that the risk of chronic SARS-CoV-2 infection is not uniform across immunosuppressive

285   conditions and provide clarity on which immunosuppression conditions predispose to delayed

286   SARS-CoV-2 RNA and culture clearance, and viral evolution. The high risk populations

287   identified in this study may benefit from targeted public health and additional therapeutic

288   interventions. In addition, the results provide further insights on the humoral and cell-mediated

289   immune correlates of viral clearance, which is crucial for the development of improved vaccines

290   and future therapies.

Materials and Methods

Participant Enrollment and Sample Collection

We enrolled participants with a positive COVID-19 test in the Mass General Brigham Medical

HealthCare System as part of the POSt-VaccInaTIon Viral CharactEristics Study (POSITIVES)

(*17, 19*) in addition to one immunocompromised participant from our previous study. Each

participant's medical record was reviewed for demographic data, immunosuppression status,

and COVID-19 treatment history by board-certified clinicians. For the POSITIVES study,

participants self-collected anterior nasal swabs every 2-3 days to a total of 6 samples over 2

weeks. Participants with immunocompromised conditions were offered to collect additional

swabs when possible and were followed until they had two consecutive negative PCR tests. For

this one immunocompromised participants reported previously(*13*), nasopharyngeal swab was

collected by healthcare providers. In a subset of participants who agreed to provide blood

sample, the first blood draw was done generally before day 15 of symptom onset (acute phase)

or first positive PCR or antigen test for COVID-19, and second blood draw between 15-60 days

after (post-acute phase) (Supplementary Fig. 5). This study was approved by Mass General

Brigham Institutional Review Board and all participants have signed informed consent upon

entry to the study.

Categorization for Immunocompromised Conditions

Immunocompromised participants were further categorized into the following groups: severe

immunocompromised participants, which were further categorized into severe-hematological

malignancy/transplant patients (S-HT), severe autoimmune patients (S-A, participants with

autoimmune condition receiving B-cell targeting agents or B cell deficiency); and non-severe

immunocompromised participants (NS). This categorization was based on a recent cohort study

which demonstrated a hierarchy of antibody response to COVID-19 vaccinations in different

medical conditions(*4, 44*). Detailed classification criteria were listed in Supplementary Table 1.

317

318   **SARS-CoV-2 Viral Load Assay**

319   SARS-CoV-2 viral RNA (vRNA) were quantified as described previously(*45*). Briefly, virions

320   were pelleted from nasal swab fluid by centrifugation at 21,000g for 2 hours at 4°C. Trizol-LS

321   Reagent (Thermo fisher Scientific, Waltham, MA) was added to the pellet, vortexed, and

322   incubated on ice for 10 minutes. Chloroform was added and the solution was vortexed before

323   centrifugation at 21,000g for 15 minutes at 4°C. RNA was isolated from the aqueous layer by

324   isopropanol precipitation and eluted in DEPC-Treated water (Thermo fisher Scientific, Waltham,

325   MA). SARS-CoV-2 RNA copies were quantified with an in-house viral load assay using the CDC

326   2019-nCoV_N1 primer and probe set (Integrated DNA Technologies, Coralville, IA). The

327   efficiency of the RNA extraction and RT-qPCR amplification was evaluated by quantifying the

328   RCAS RNA recovered from each sample and the two N1 controls. The importin-8 (IPO8) human

329   housekeeping gene was also amplified and evaluated as a measure of sample collection

330   quality. Samples were run in triplicate wells for N1, and in duplicate wells for RCAS and IPO8.

331

332   **SARS-CoV-2 Viral Culture Assay**

333   Viral culture was performed as previously reported(*17*). Vero-E6 cells (ATCC, Manassas, VA)

334   maintained in DMEM (Corning, Corning, NY) supplemented with HEPES (Corning, Corning,

335   NY), 1X Penicillin (100 IU/mL)/Streptomycin (100 µg/ml) (Corning, Corning, NY), 1X Glutamine

336   (Glutamax, Thermo fisher Scientific, Waltham, MA) and 10% FBS (MilliporeSigma, Burlington,

337   MA) were plated 16-20 hours before infection. Each sample consisting of nasal swab fluid was

338   thawed on ice and filtered through a Spin-X 0.45 um filter (Corning, Corning, NY) at 10,000 xg

339   for 5 minutes. Before infection the media was changed to DMEM supplemented with HEPES,

340   1X Antibiotic/Antimycotic (Thermo Fisher, Waltham, MA), 1X Glutamine, 2% FBS and 5 µg/mL

341   of polybrene (Santa Cruz Biotechnologies, Dallas, TX). Each filtered sample was then used to

342   inoculate Vero-E6 cells by spinfection (2,000x g for 1 hour at 37C). Each condition was plated in

343   quadruplicate wells in 1:5 dilutions across half the plate. The plates were observed at 7-days

344   post-infection using a light microscope to check for cytopathogenic effect (CPE) and a median

345   tissue culture infectious dose ($TCID_{50}$) was calculated for each sample.

346

347   **Neutralizing Antibody Responses**

348   Neutralizing activity against SARS-CoV-2 pseudovirus was measured using a single-round

349   infection assay in 293T/ACE2 target cells(*18*). Pseudotyped virus particles were produced in

350   293T/17 cells (ATCC, Manassas, VA) by co-transfection of plasmids encoding codon-optimized

351   full-length Spike (ancestral-D614G, Delta, Omicron-BA.1, Omicron-BA.2, Omicron-BA.4/5),

352   packaging plasmid pCMV ΔR8.2, and luciferase reporter plasmid pHR' CMV-Luc. Packaging

353   and luciferase plasmids were kindly provided by Dr. Barney Graham (NIH, Vaccine Research

354   Center). The 293T cell line stably overexpressing the human ACE2 cell surface receptor protein

355   was kindly provided by Drs. Michael Farzan and Huihui Ma (The Scripps Research Institute).

356   For neutralization assays, serial dilutions of patient sera were performed in duplicate followed by

357   addition of pseudovirus. Pooled serum samples from convalescent COVID-19 patients or pre-

358   pandemic normal healthy serum (NHS) were used as positive and negative controls,

359   respectively. Plates were incubated for 1 hour at 37℃ followed by addition of 293/ACE2 target

360   cells ($1x10^4$/well). Wells containing cells + pseudovirus (without sample) or cells alone acted as

361   positive and negative infection controls, respectively. Assays were harvested on day 3 using

362   Promega BrightGlo luciferase reagent and luminescence detected with a Promega GloMax

363   luminometer (Promega, Madison, WI). Titers are reported as the dilution of serum that inhibited

364   50% virus infection (ID_{50} titer). Pseudovirus-based neutralization assays were conducted using

365   ancestral Spike protein, as well as Delta- and Omicron- (BA.1, BA.2, or BA.4/5) Spike. Anti-

366   variant neutralizing antibody level (nAb) was determined based on the viral strain each

367 participant was infected with (either by sequencing or in small proportion, imputed by time of

368 infection when specific strain was prevalent).

369

370 **Nucleocapsid binding antibody assay**

371 Binding antibody against Nucleocapsid protein was measured using Coronavirus Ig Total

372 Human 11-Plex ProcartaPlex™ Panel (Thermo fisher Scientific, Waltham, MA) according to the

373 manufacturer's instruction.

374

375 **T Cell Enzyme-linked immunosorbent spot (ELISpot) Assay**

376 Interferon (IFN)-γ ELISpot assay was reported in our previous study and were performed

377 according to the manufacturer's instructions (Mabtech, Cincinnati, OH)(*46*). Briefly, peripheral

378 blood mononuclear cells (PBMCs) were incubated with SARS-CoV-2 peptide pools (MGH

379 Peptide Core) at a final concentration of 0.5μg/ ml for 16–18h (100,000-200,000 cells per test).

380 Anti-CD3 (Clone OKT3, Biolegend, 0.5μg/mL, San Diego, CA) and anti-CD28 Ab (Clone

381 CD28.2, Biolegend, 0.5μg/mL, San Diego, CA) were used as positive controls. To quantify

382 antigen-specific responses, mean spots of the DMSO negative control wells were subtracted

383 from the positive wells. The results were expressed as spot-forming units (SFU) per 10^6

384 PBMCs. Responses were considered positive if the results were >5 SFU/10^6 PBMCs following

385 control subtraction. If negative DMSO control wells had >30 SFU/10^6 PBMCs or if positive

386 control wells (anti-CD3/anti-CD28 stimulation) did not have >1000 spot-forming units, the results

387 were deemed invalid and excluded from further analysis.

388

389 **T Cell Proliferation Assay**

390 T Cell proliferation assay was reported previously(*46*). Briefly, PBMCs were incubated in PBS

391 with 0.5 uM carboxyfluorescein succinimidyl ester (CFSE; Life Technologies, Carlsbad, CA) or

392 CellTrace™ Far Red (CTFR, Invitrogen, Waltham, MA) at 37°C for 20 min. Then they were

393   washed and resuspended at 0.5-1 × 10^6/mL and plated into 96-well U-bottom plates (Corning) in

394   200 µL of. media. Peptide pools were added at a final concentration of 0.5 µg/mL, followed by

395   incubation at 37°C, 5% CO_2 for six days. The PBMC staining antibody panels are in

396   Supplementary Materials. Cells were washed and fixed in 2% paraformaldehyde prior to flow

397   cytometric analysis on a BD LSR II (BD Biosciences, Franklin Lakes, NJ). A positive

398   proliferation response was defined as a percentage of $CD3^+CD4^+$ or $CD3^+CD8^+$ $CFSE^{low}$ or

399    $CTFR^{low}$ cells with at least 1.5x greater than the highest of two negative-control wells and

400   greater than 0.2% $CFSE^{low}$ or $CTFR^{low}$ cells in magnitude following background subtraction.

401

402   **SARS-CoV-2 S-gene Sequencing**

403   SARS-CoV-2 viral RNA (vRNA) isolation as described previously(*45*). RNA was converted to

404   cDNA using Superscript IV reverse transcriptase (Invitrogen, Waltham, MA) as per manufacturer's

405   instructions). Spike (S) gene amplification was performed using a nested PCR strategy with in-

406   house designed primer sets targeting codons 1–814 of the Spike as previously described(*28*).

407   Further, PCR products from different individuals were pooled, and Illumina library construction

408   was performed using the Nextera XT library prep kit (Illumina). Sequencing was performed on the

409   Illumina MiSeq platform and deep sequencing data analysis was carried out using the Stanford

410   Coronavirus   Antiviral   &   Resistance   Database   (CoVDB)   platform

411   (https://covdb.stanford.edu/sierra/sars2/by-reads/?cutoff=0.01&mixrate=0.01)(*47*). Input FASTQ

412   sequence alignment with Wuhan-Hu-1 reference was done using MiniMap2 version 2.22 in

413   CodFreq pipeline (https://github.com/hivdb/codfreq). The output of MiniMap2, an aligned SAM

414   file, is converted to a CodFreq file by an in-house written Python script using a PySam library

415   (version: 0.18.0) and further analyzed with the CoVDB. PCR and sequencing runs were

416   performed once with the appropriate positive and negative controls. For S gene analysis, amino

417   acid variants were then called at the codon level using perl code and used for resistance

418   interpretation with a 1% limit of detection. The accuracy of the deep sequencing platforms was

419   evaluated with a control library of clonal SARS-CoV-2 sequences mixed at known concentrations

420   as described previously(*48*). Mutations detected by next-generation sequencing at <20% of the

421   viral population were labelled as 'low-frequency' variants as they would largely be missed by

422   traditional Sanger sequencing. A minimum average of 500x sequencing coverage per sample

423   was required for variant calling. SARS-COV-2 variant calling was done using 3 different variant

424   calling platforms, namely, CoVDB(*47*), Scorpio call v1.2.123 (https://pangolin.cog-uk.io/), and

425   Nextclade v.1.13.2 (https://clades.nextstrain.org/)(*49*).

426

427   **Single nucleotide variation, and genetic diversity analysis**

428   For assessing intrahost single nucleotide variation (iSNV), data from only those participants were

429   included for whom sequence data from baseline and at least one follow-up time point were

430   available. SNV analysis was performed using PASeq SARS-CoV-2 pipeline (www.paseq.org).

431   Briefly, raw sequence files were quality filtered and adapter-trimmed using trimmomatic (v0.30).

432   Contaminating sequences were filtered out using BBMap Suite (v35.76). Duplicated reads were

433   detected using fastuniq (v1.1). High quality non-redundant reads were then aligned to SARS-

434   CoV-2 Wuhan reference (NC_045512.2) using Bowtie2 (v.2.3.2). Resulting alignments were

435   processed with samtools (v.1.2) and iVar (v1.4.2) to obtain nucleotide variant VCF files.

436   Nucleotide variants present at 100% frequency of the total viral population at all time points

437   indicative of lineage defining mutations were excluded from the iSNV analysis. Genetic diversity

438   between multiple sequences of an individual were assessed by average pairwise distance in

439   MEGA both at the nucleotide and amino-acid level.

440

441   **Statistical Analysis**

442   Categorical variables were summarized using total number and percentage and between-group

443   differences were evaluated using either chi-squared test or Fisher's exact test when

444   appropriate. Continuous variables were summarized with median and interquartile ranges and

445   compared with non-parametric methods (Wilcoxon rank-sum test to compare two groups and

446   Dunn's test with Benjamini-Hochberg adjustment to compare three or more groups). Within

447   group comparison was conducted using paired Wilcoxon signed-rank test without adjustment for

448   multiple comparisons. We also used generalized estimating equation (GEE) with Gaussian

449   estimation to evaluate between-group differences accounting for repeated measurement during

450   longitudinal follow-up. R (4.3.0) was used for statistical analyses. Two-tailed tests were used for

451   all the analyses and P<0.05 was considered statistically significant unless specified otherwise.

452

453   **List of Supplementary Materials**

454   Supplementary Methods

455   Supplementary Tables 1-3

456   Supplementary Figures 1-5

Authors Contribution

Study conceptualization: MJ Siedner, AK Barczak, JE Lemieux, JZ Li

First draft writing: Y Li, MC Choudhary, J Regan, JZ Li

Draft review, discussion and approval: All authors

Statistical analyses: Y Li, MC Choudhary, R Deo, J Regan

Chart review and participant classification: Y Li, Y Kawano, ZS Wallace, JA Sparks

Virology assays: J Regan, J Boucau, GE Edelstein, C Marino, JP Flynn

Sequencing analyses: MC Choudhary, R Uddin, R Deo, JE Lemieux, JZ Li

483   Neutralizing antibody assays: T Speidel, MS Seaman

484   Binding antibody assays: MY Liew

485   T cell assays: A Nathan, MA Getz, GD Gaiha

486   Study coordination, sample collection, participant referral: Z Reynold, M Barry, RF Gilbert, D
487   Tien, S Sagar, TD Vyas, SP Hammond, LA Novack, B Choi, M Cernadas, ZS Wallace, JA
488   Sparks, JM Vyas

489   Database management: MJ Siedner, RF Gilbert

490

References

1. H. M. El Sahly *et al.*, Efficacy of the mRNA-1273 SARS-CoV-2 Vaccine at Completion of Blinded Phase. *N Engl J Med* **385**, 1774-1785 (2021).

2. E. D. Moreira, Jr. *et al.*, Safety and Efficacy of a Third Dose of BNT162b2 Covid-19 Vaccine. *N Engl J Med* **386**, 1910-1921 (2022).

3. O. J. Watson *et al.*, Global impact of the first year of COVID-19 vaccination: a mathematical modelling study. *Lancet Infect Dis* **22**, 1293-1302 (2022).

4. G. Haidar *et al.*, Prospective Evaluation of Coronavirus Disease 2019 (COVID-19) Vaccine Responses Across a Broad Spectrum of Immunocompromising Conditions: the COVID-19 Vaccination in the Immunocompromised Study (COVICS). *Clin Infect Dis* **75**, e630-e644 (2022).

5. L. Wieske *et al.*, Humoral responses after second and third SARS-CoV-2 vaccination in patients with immune-mediated inflammatory disorders on immunosuppressants: a cohort study. *Lancet Rheumatol* **4**, e338-e350 (2022).

6. J. D. Kelly *et al.*, Incidence of Severe COVID-19 Illness Following Vaccination and Booster With BNT162b2, mRNA-1273, and Ad26.COV2.S Vaccines. *JAMA* **328**, 1427-1437 (2022).

7. U. Agrawal *et al.*, Severe COVID-19 outcomes after full vaccination of primary schedule and initial boosters: pooled analysis of national prospective cohort studies of 30 million individuals in England, Northern Ireland, Scotland, and Wales. *Lancet* **400**, 1305-1320 (2022).

8. D. Planas *et al.*, Reduced sensitivity of SARS-CoV-2 variant Delta to antibody neutralization. *Nature* **596**, 276-280 (2021).

9. M. Hoffmann *et al.*, SARS-CoV-2 variant B.1.617 is resistant to bamlanivimab and evades antibodies induced by infection and vaccination. *Cell Reports* **36**, (2021).

10. Q. Wang *et al.*, Antibody evasion by SARS-CoV-2 Omicron subvariants BA.2.12.1, BA.4 and BA.5. *Nature* **608**, 603-608 (2022).

11. S. Weigang *et al.*, Within-host evolution of SARS-CoV-2 in an immunosuppressed COVID-19 patient as a source of immune escape variants. *Nat Commun* **12**, 6405 (2021).

12. S. Cele *et al.*, SARS-CoV-2 prolonged infection during advanced HIV disease evolves extensive immune escape. *Cell Host Microbe* **30**, 154-162 e155 (2022).

13. B. Choi *et al.*, Persistence and Evolution of SARS-CoV-2 in an Immunocompromised Host. *N Engl J Med* **383**, 2291-2293 (2020).

525 14. M. K. Hensley *et al.*, Intractable Coronavirus Disease 2019 (COVID-19) and Prolonged
526   Severe Acute Respiratory Syndrome Coronavirus 2 (SARS-CoV-2) Replication in a
527   Chimeric Antigen Receptor-Modified T-Cell Therapy Recipient: A Case Study. *Clin Infect*
528   *Dis* **73**, e815-e821 (2021).

529 15. S. Harari *et al.*, Drivers of adaptive evolution during chronic SARS-CoV-2 infections. *Nat*
530   *Med* **28**, 1501-1508 (2022).

531 16. M. C. Choudhary, C. R. Crain, X. Qiu, W. Hanage, J. Z. Li, Severe Acute Respiratory
532   Syndrome Coronavirus 2 (SARS-CoV-2) Sequence Characteristics of Coronavirus
533   Disease 2019 (COVID-19) Persistence and Reinfection. *Clin Infect Dis* **74**, 237-245
534   (2022).

535 17. J. Boucau *et al.*, Duration of Shedding of Culturable Virus in SARS-CoV-2 Omicron
536   (BA.1) Infection. *N Engl J Med* **387**, 275-277 (2022).

537 18. M. S. Seaman *et al.*, Vaccine breakthrough infection leads to distinct profiles of
538   neutralizing antibody responses by SARS-CoV-2 variant. *JCI Insight* **7**, (2022).

539 19. M. J. Siedner *et al.*, Duration of viral shedding and culture positivity with postvaccination
540   SARS-CoV-2 delta variant infections. *JCI Insight* **7**, (2022).

541 20. V. A. Avanzato *et al.*, Case Study: Prolonged Infectious SARS-CoV-2 Shedding from an
542   Asymptomatic Immunocompromised Individual with Cancer. *Cell* **183**, 1901-1912.e1909
543   (2020).

544 21. C. Chaguza *et al.*, Accelerated SARS-CoV-2 intrahost evolution leading to distinct
545   genotypes during chronic infection. *Cell Rep Med* **4**, 100943 (2023).

546 22. B. Bailly *et al.*, Persistent Coronavirus Disease 2019 (COVID-19) in an
547   Immunocompromised Host Treated by Severe Acute Respiratory Syndrome Coronavirus
548   2 (SARS-CoV-2)-Specific Monoclonal Antibodies. *Clin Infect Dis* **74**, 1706-1707 (2022).

549 23. A. Truffot *et al.*, SARS-CoV-2 Variants in Immunocompromised Patient Given Antibody
550   Monotherapy. *Emerg Infect Dis* **27**, 2725-2728 (2021).

551 24. A. Gupta *et al.*, Host immunological responses facilitate development of SARS-CoV-2
552   mutations in patients receiving monoclonal antibody treatments. *J Clin Invest* **133**,
553   (2023).

554 25. J. H. Baang *et al.*, Prolonged Severe Acute Respiratory Syndrome Coronavirus 2
555   Replication in an Immunocompromised Patient. *J Infect Dis* **223**, 23-27 (2021).

556 26. Y. Bronstein *et al.*, Evolution of spike mutations following antibody treatment in two
557   immunocompromised patients with persistent COVID-19 infection. *J Med Virol* **94**, 1241-
558   1245 (2022).

27. A. S. Gonzalez-Reiche *et al.*, Sequential intrahost evolution and onward transmission of SARS-CoV-2 variants. *Nat Commun* **14**, 3235 (2023).

28. M. C. Choudhary *et al.*, Emergence of SARS-CoV-2 escape mutations during Bamlanivimab therapy in a phase II randomized clinical trial. *Nat Microbiol* **7**, 1906-1917 (2022).

29. S. A. Kemp *et al.*, SARS-CoV-2 evolution during treatment of chronic infection. *Nature* **592**, 277-282 (2021).

30. S. A. Apostolidis *et al.*, Cellular and humoral immune responses following SARS-CoV-2 mRNA vaccination in patients with multiple sclerosis on anti-CD20 therapy. *Nat Med* **27**, 1990-2001 (2021).

31. V. Dioverti, S. Salto-Alejandre, G. Haidar, Immunocompromised Patients with Protracted COVID-19: a Review of "Long Persisters". *Curr Transplant Rep*, 1-10 (2022).

32. V. Nussenblatt *et al.*, Yearlong COVID-19 Infection Reveals Within-Host Evolution of SARS-CoV-2 in a Patient With B-Cell Depletion. *J Infect Dis* **225**, 1118-1123 (2022).

33. T. Aydillo *et al.*, Shedding of Viable SARS-CoV-2 after Immunosuppressive Therapy for Cancer. *N Engl J Med* **383**, 2586-2588 (2020).

34. S. Gandhi *et al.*, De novo emergence of a remdesivir resistance mutation during treatment of persistent SARS-CoV-2 infection in an immunocompromised patient: a case report. *Nat Commun* **13**, 1547 (2022).

35. C. L. Gordon *et al.*, Defective Severe Acute Respiratory Syndrome Coronavirus 2 Immune Responses in an Immunocompromised Individual With Prolonged Viral Replication. *Open Forum Infect Dis* **8**, ofab359 (2021).

36. I. Monrad *et al.*, Persistent Severe Acute Respiratory Syndrome Coronavirus 2 Infection in Immunocompromised Host Displaying Treatment Induced Viral Evolution. *Open Forum Infect Dis* **8**, ofab295 (2021).

37. K. M. Braun *et al.*, Acute SARS-CoV-2 infections harbor limited within-host diversity and transmit via tight transmission bottlenecks. *PLoS Pathog* **17**, e1009849 (2021).

38. K. K. K. Ko *et al.*, Emergence of SARS-CoV-2 Spike Mutations during Prolonged Infection in Immunocompromised Hosts. *Microbiol Spectr* **10**, e0079122 (2022).

39. K. A. Lythgoe *et al.*, SARS-CoV-2 within-host diversity and transmission. *Science* **372**, (2021).

40. A. L. Valesano *et al.*, Temporal dynamics of SARS-CoV-2 mutation accumulation within and across infected hosts. *PLoS Pathog* **17**, e1009499 (2021).

592   41.   A. Soresina *et al.*, Two X-linked agammaglobulinemia patients develop pneumonia as
593   COVID-19 manifestation but recover. *Pediatr Allergy Immunol* **31**, 565-569 (2020).

594   42.   T. Dangi *et al.*, Improved control of SARS-CoV-2 by treatment with nucleocapsid-specific
595   monoclonal antibody. *J Clin Invest*, e162282 [Online ahead of print] (2022).

596   43.   R. Kundu *et al.*, Cross-reactive memory T cells associate with protection against SARS-
597   CoV-2 infection in COVID-19 contacts. *Nat Commun* **13**, 80 (2022).

598   44.   K. Maneikis *et al.*, Immunogenicity of the BNT162b2 COVID-19 mRNA vaccine and early
599   clinical outcomes in patients with haematological malignancies in Lithuania: a national
600   prospective cohort study. *The Lancet Haematology* **8**, e583-e592 (2021).

601   45.   J. Fajnzylber *et al.*, SARS-CoV-2 viral load is associated with increased disease severity
602   and mortality. *Nat Commun* **11**, 5493 (2020).

603   46.   A. Nathan *et al.*, Structure-guided T cell vaccine design for SARS-CoV-2 variants and
604   sarbecoviruses. *Cell* **184**, 4401-4413.e4410 (2021).

605   47.   P. L. Tzou, K. Tao, S. L. K. Pond, R. W. Shafer, Coronavirus Resistance Database
606   (CoV-RDB): SARS-CoV-2 susceptibility to monoclonal antibodies, convalescent plasma,
607   and plasma from vaccinated persons. *PLoS One* **17**, e0261045 (2022).

608   48.   J. Z. Li *et al.*, Impact of pre-existing drug resistance on risk of virological failure in South
609   Africa. *J Antimicrob Chemother* **76**, 1558-1563 (2021).

610   49.   I. Aksamentov, C. Roemer, E. B. Hodcroft, R. A. Neher, Nextclade: clade assignment,
611   mutation calling andquality control for viral genomes. *The Journal of Open Source*
612   *Software* **6**, 3773 (2021).

613

614

615 **Figure Legends**

616 **Figure 1. Kinetics of SARS-CoV-2 viral RNA and culturable virus among different**

617 **immunocompromised groups. a**, Upper respiratory viral load decay. Lower level of

618 quantification (LLOQ) is 10 copies/ml. **b**, Kaplan-Meier estimates of upper respiratory viral

619 clearance (viral load below LLOQ). **c**, Upper respiratory culturable virus dynamics (50% Tissue

620 Culture Infectious Dose [$TCID_{50}$]). **d**, Kaplan-Meier estimates of upper respiratory culturable

621 virus clearance.

622

623 **Figure 2. SARS-CoV-2 intra-host mutations among different immunocompromise groups.**

624 **a,** Number of intra-host single-nucleotide variants (iSNVs) among severe (S-HT in red and S-A

625 in green), non-severe immunocompromised and non-immunocompromised (None) groups. **b,**

626 Nucleotide average pairwise distance (APD) among severe (S-HT in red and S-A in green),

627 non-severe immunocompromised (NS) and non-immunocompromised (None) groups. **c,**

628 Participants with any nucleotide changes during follow-up. **d**, Heat map showing distribution of

629 Spike polymorphisms from participants receiving mAb treatment. Each row represents one

630 participant, while x axis shows amino acid positions in the Spike gene. Different domains of

631 Spike are shown at the top. Colors indicate frequency of polymorphisms, with blue indicating the

632 lowest value and red indicating the highest value in the scale. Participants in different study

633 groups are separated by a red horizontal line. **e**, Proportion of mAb resistance emergence

634 amongst those treated with mAbs, categorized by those with severe or non-severe/no

635 immunosuppression. Comparison of iSNV and APD between groups were done using using

636 Dunn's test with Benjamini-Hochberg P value adjustment. Fisher's exact test was used to

637 calculate significance between participants with and without viral evolution and further, in

638 participants with and without mAb treatment specific resistance mutations. Only significant P

639 values are shown. NTD, N-terminal domain; RBD, receptor binding domain; RBM, receptor

640 binding motif; S1, subunit 1; S2, subunit 2.

641

642 **Figure 3. Neutralizing antibody (nAb) and Nucleocapsid binding antibody levels among**

643 **different immunocompromised groups. a**, nAb levels (50% inhibitory dilution [ID_{50}]) against

644 ancestral Spike protein. **b**, nAb levels against variant-specific Spike protein. **c** and **d**,

645 Longitudinal trajectory of nAb in different immunocompromise groups, including (**c**) or excluding

646 (**d**) monoclonal antibody use. **e**, binding antibody levels against Nucleocapsid protein. **f**,

647 Longitudinal trajectory of binding antibody in different immunocompromise groups. Comparison

648 between different immunocompromise groups at the same time point was performed using

649 Dunn's test with Benjamini-Hochberg P value adjustment. Comparison of longitudinal antibody

650 changes for participants with two blood draws was performed using the pairwise Wilcoxon rank

651 sum test with Benjamini-Hochberg P value adjustment. Only significant P values were shown.

652 Tukey boxplot was used to summarize antibody levels. Generalized additive model was used to

653 evaluate the trend of antibody development with 95% confidence intervals in the shaded area.

654 Lines between two timepoints indicate the same participants with two blood draws. S-HT,

655 severe hematologic-oncology/transplant; S-A, severe autoimmune/B-cell deficient; NS, non-

656 severe. Severe group included both S-HT and S-A as they had comparable antibody levels at

657 multiple time points.

658

659 **Figure 4. Spike-specific T levels among different immunocompromised groups. a**,

660 enzyme-linked immunosorbent spot (ELIspot) assays using peptide pools derived from

661 ancestral and variant-specific Spike protein. **b, c**, $CD4^+$ T cell (b) and $CD8^+$ T cell proliferation

662 (c) upon stimulation of ancestral- and variant-specific Spike peptide pools. **d**, Longitudinal

663 trajectory of Spike-specific T levels in different immunocompromise groups. Comparison

664 between different immunocompromise groups at the same time point was performed using

665 Dunn's test with Benjamini-Hochberg P value adjustment. Comparison of longitudinal antibody

666 changes for participants with two blood draws was performed using the pairwise Wilcoxon rank

667   sum test with Benjamini-Hochberg P value adjustment. Only significant P values were shown.

668   Tukey boxplot was used to summarize antibody levels. Generalized additive model was used to

669   evaluate the trend of antibody development with 95% confidence intervals in the shade area.

670   Lines between two timepoints indicate the same participants with two blood draws.

671

672

Table 1. Demographic and clinical information.

	Immunocompromised (N=56)	Non-Immunocompromised (N=184)	Total (N=240)	P value
Sex, n (%)				0.2
Female	32 (57.1%)	126 (68.5%)	158 (65.8%)	
Male	24 (42.9%)	58 (31.5%)	82 (34.2%)	
Age, Median (Q1, Q3)	55 (45, 67)	46 (33, 59)	49 (34-60)	0.001
Race, n (%)				0.8
Asian	1 (1.8)	10 (5.4)	11 (4.6)	
Black or AA	5 (8.9)	19 (10.3)	24 (10.0)	
Other/Unknown	5 (8.9)	16 (8.7)	21 (8.8)	
White	45 (80.4)	139 (75.5)	184 (76.7)	
Ethnicity				0.5
Hispanic or Latino	5 (8.9)	17 (9.2)	22 (9.2)	
Not Hispanic or Latino	47 (83.9)	143 (77.7)	190 (79.2)	
Other/Unknown	4 (7.1)	24 (13.0)	28 (11.7)	
Inpatient, n (%)	7 (12.5)	8 (4.3)	15 (6.2)	0.051
Number of vaccinations, median number, (Q1, Q3)	3 (3-4)	3 (2-3)	3 (2-4)	<0.001
mAb use, n (%)	24* (42.9)	10 (5.4)	34 (14.2)	<0.001
Antiviral use, n (%)	40 (71.4)	57 (31.0)	97 (40.4)	<0.001
Immunocompromise group, n (%)				<0.001
S-HT	12 (21.4)	0 (0.0)	12 (5.0)	
S-A	13 (23.2)	0 (0.0)	13 (5.4)	
NS	31 (55.4)	0 (0.0)	31 (12.9)	
None	0 (0.0)	184 (100.0)	184 (76.7)	
Symptom duration, median days** (Q1, Q3)	5 (4, 7)	4 (3, 6)	4 (3, 6)	0.04
Variant***				<0.001
Delta	3 (5.4)	43 (23.4)	46 (19.2)	
Omicron	48 (85.7)	137 (74.5)	185 (77.1)	
Other/Unknown	5 (8.9)	4 (2.2)	9 (3.8)	

Q1 and Q3, quartile 1 and quartile 3; AA, African American; mAb, monoclonal antibody; S-HT, severe with malignant hematology or transplant history; S-A, severe autoimmune/B-cell deficient; NS, non-severe immunocompromising condition.

*, four participants received Mab after blood draws.

**, Symptom duration indicates the duration between symptom onset (patient report or first positive test if asymptomatic screening) and first nasal swab collected by the study group.

***, Variant information was obtained by either Spike or whole genome sequencing or by epidemiological information (time period when the participant was infected).

Table 2. Association between immunocompromise groups and SARS-CoV-2 viral decay.

Hazard ratio for SARS-CoV-2 viral RNA clearance				
Group	HR (95% CI)	P	aHR (95% CI)	P
None (Reference)				
S-HT	0.22 (0.09-0.52)	0.0005	0.32 (0.12-0.83)	0.02
S-A	0.64 (0.34-1.22)	0.2	0.74 (0.33-1.64)	0.5
NS	0.82 (0.54-1.24)	0.4	0.92 (0.58-1.46)	0.7
Hazard ratio for SARS-CoV-2 culturable virus clearance				
Group	HR (95% CI)	P	aHR (95% CI)	P
None (Reference)				
S-HT	0.23 (0.11-0.48)	8.7E-5	0.27 (0.12-0.63)	0.002
S-A	0.54 (0.28-1.03)	0.06	0.53 (0.26-1.11)	0.09
NS	1.12 (0.76-1.66)	0.6	1.35 (0.89-2.06)	0.2

HR, hazard ratio; aHR, adjusted hazard ratio; CI, confidence interval.

Age, sex at birth, race, ethnicity, number of vaccinations, monoclonal use, and antiviral use were adjusted for in the multivariate models.
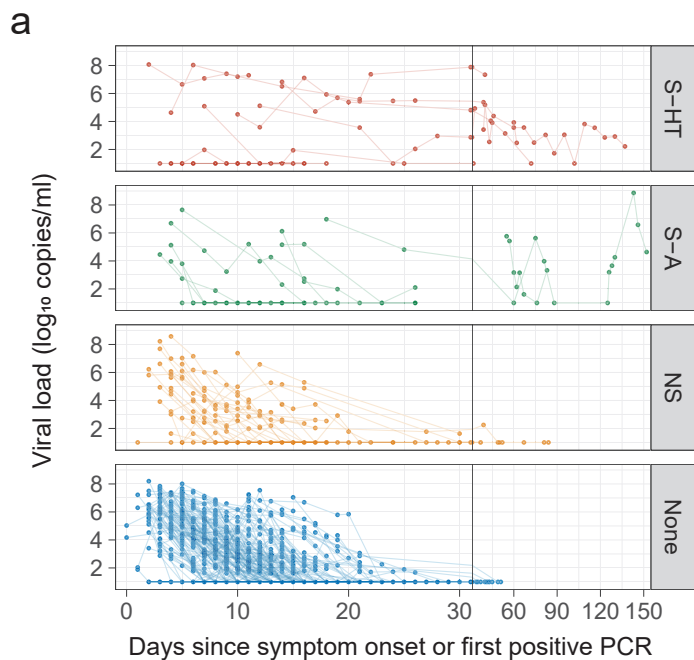
Figure 1
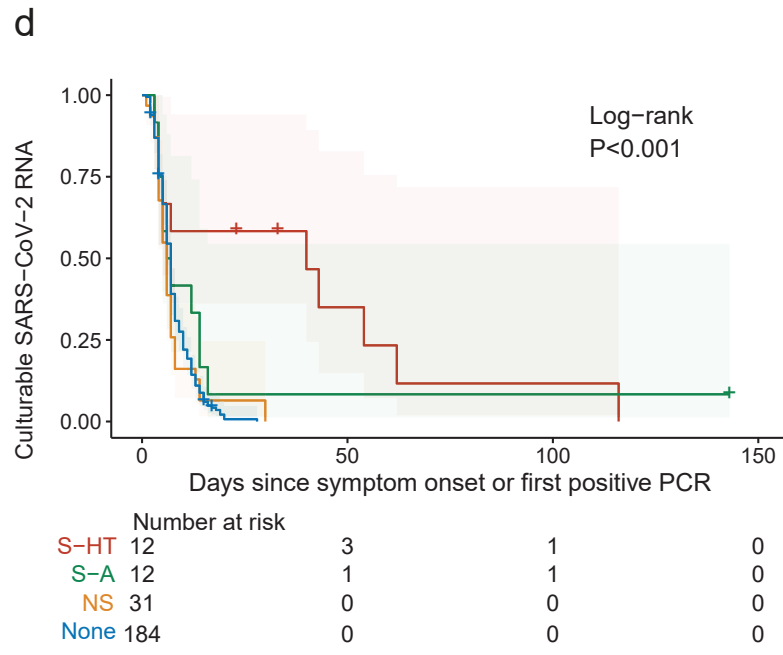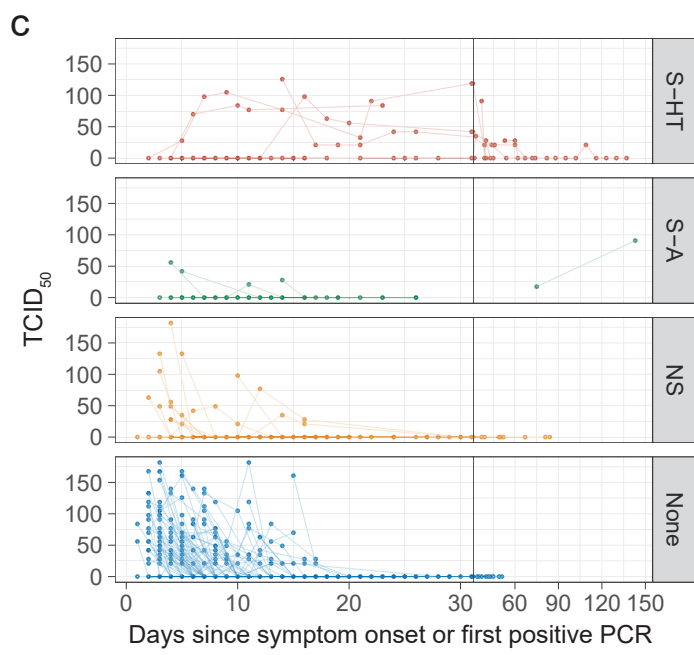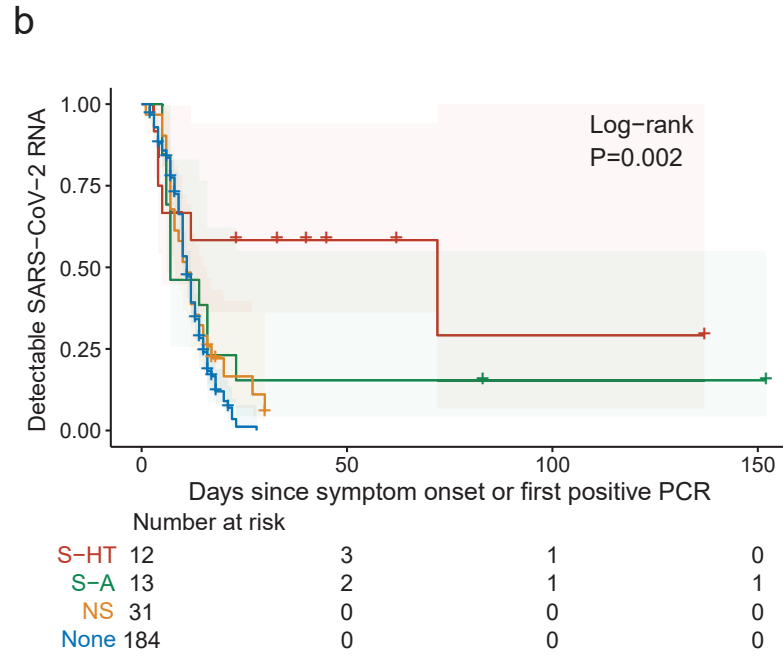
Figure 2
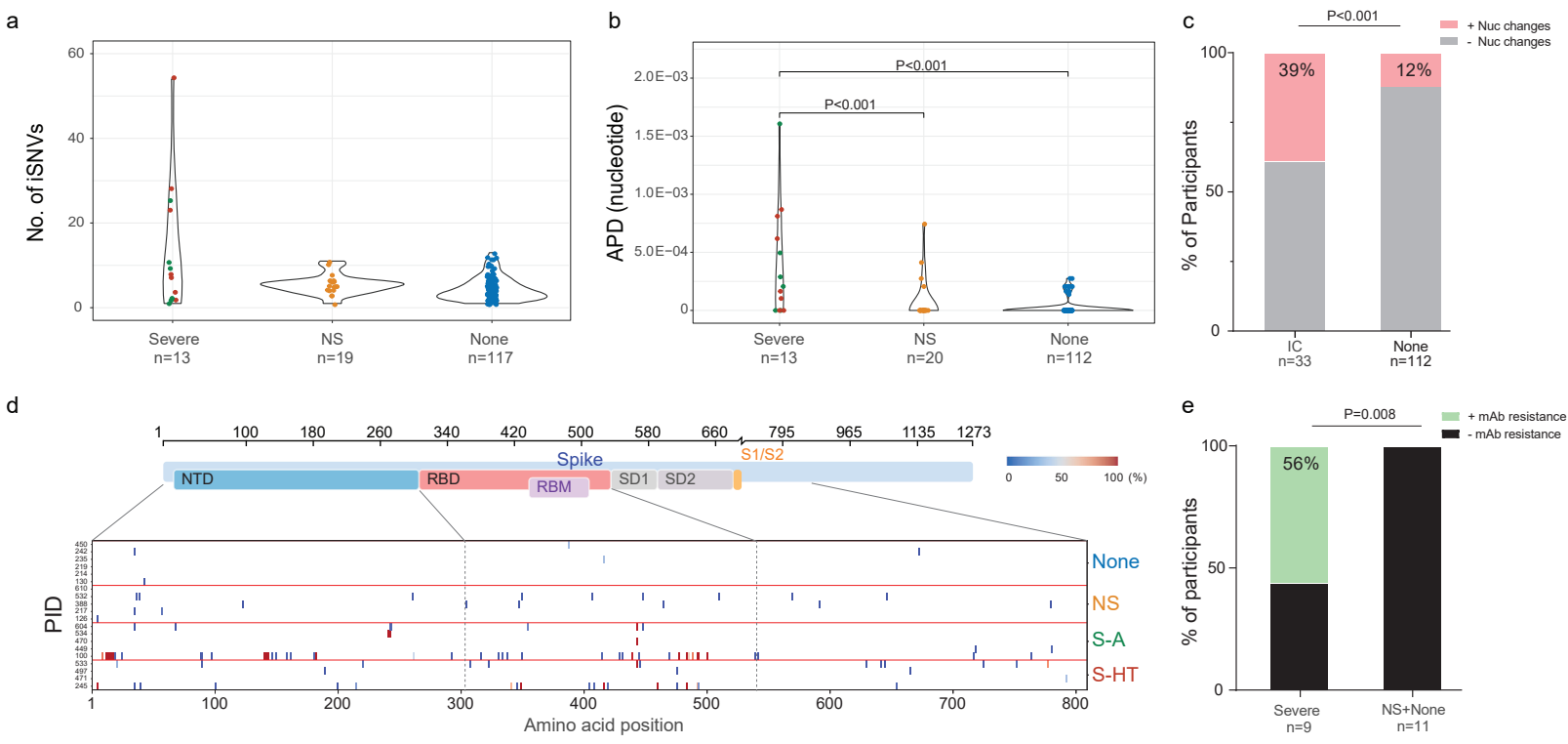
Figure 3
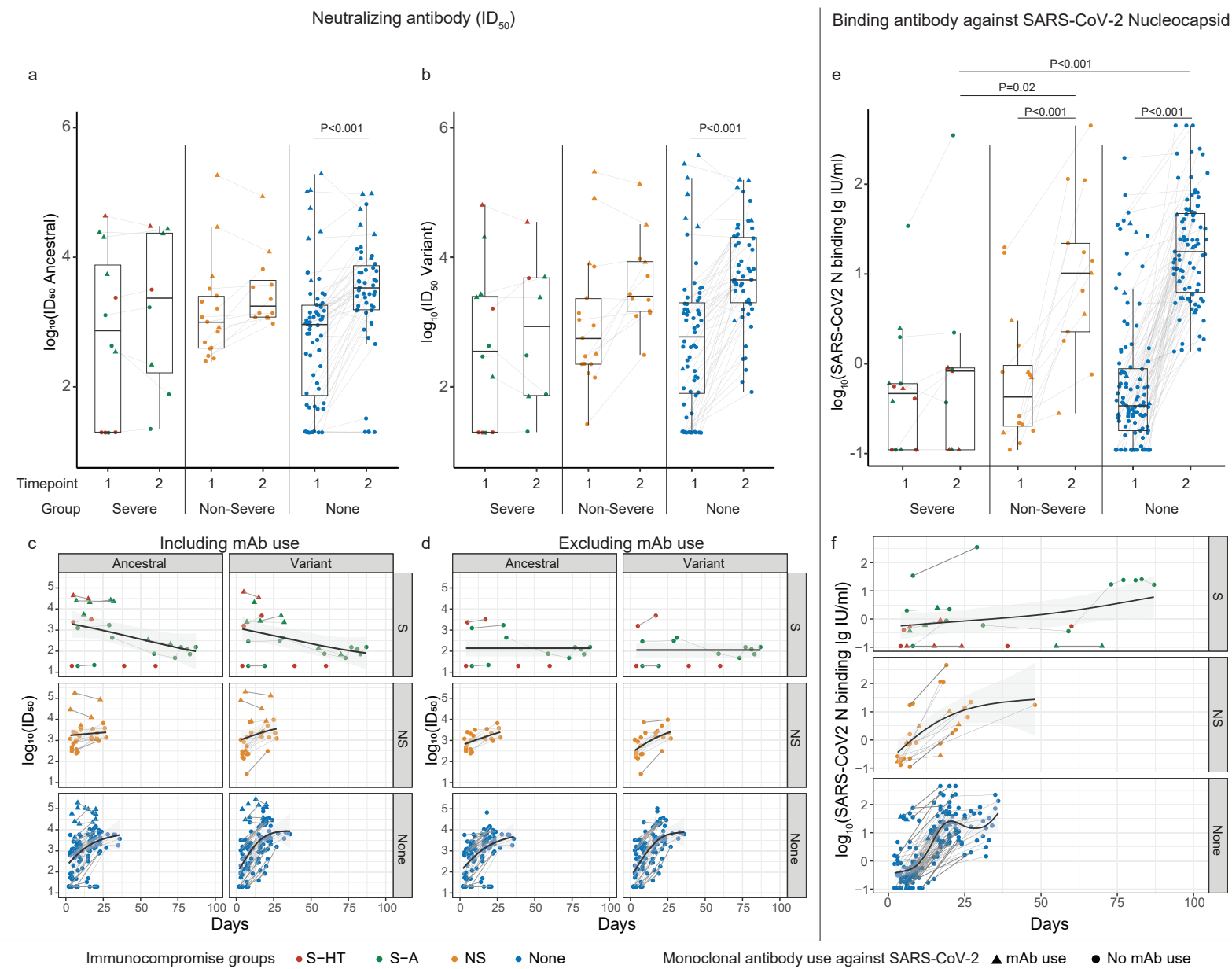
Figure 4
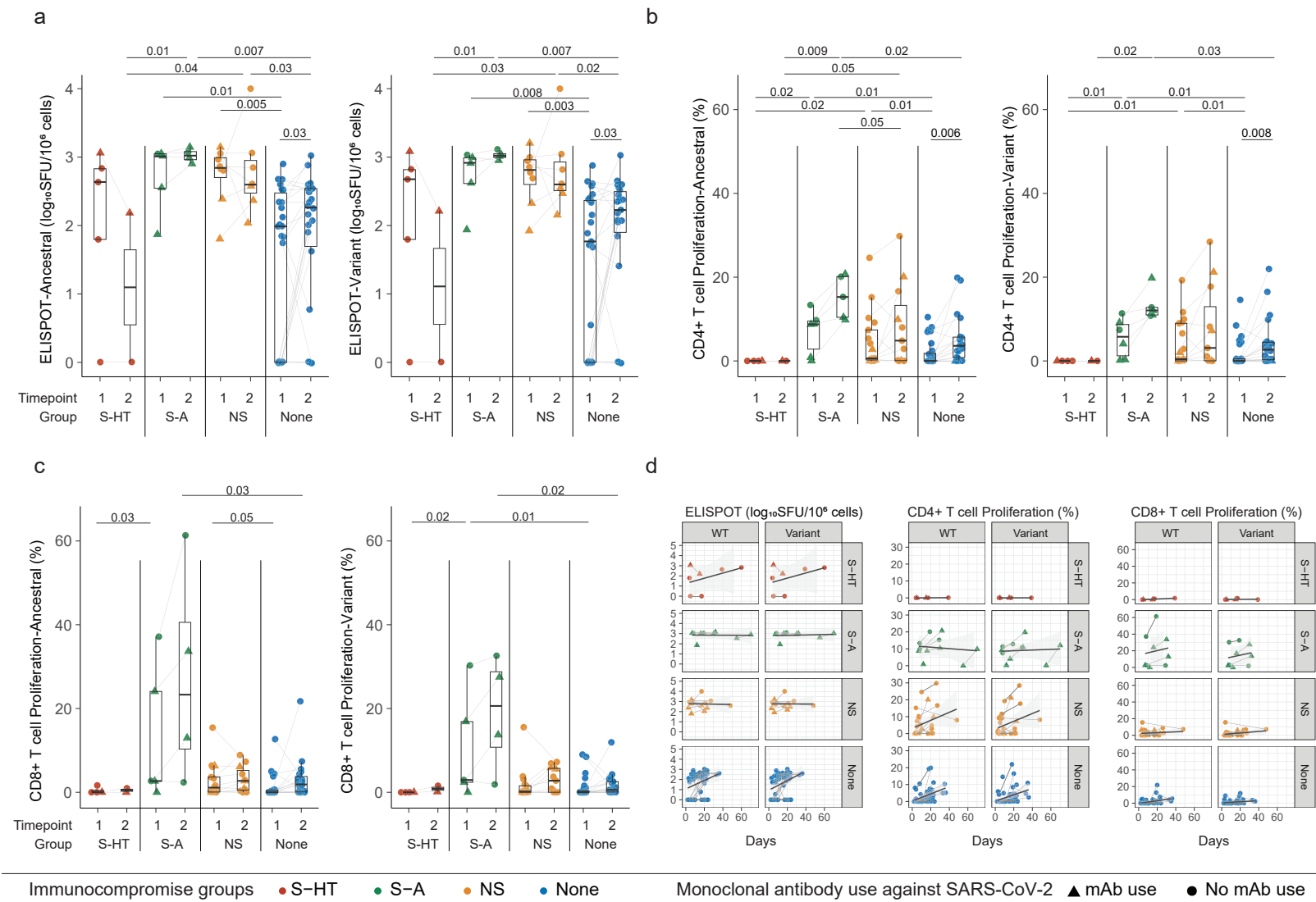
Supplementary Materials

Supplementary Methods

T cell proliferation staining panels

For PBMCs stained with carboxyfluorescein succinimidyl ester (CFSE; Life Technologies), cells were then washed and stained with anti-CD3 PE-Cy7 (clone SK7; BioLegend), anti-CD8 APC (clone SK1; BioLegend), anti-CD4 BV711 (clone RPA-T4; BioLegend), and LIVE/DEAD violet viability dye (Life Technologies).

For PBMCs stained with Cell Trace Far Red Proliferation Dye (CTFR, Invitrogen), cells were then washed and stained with anti-CD3 APC-Cy7 (clone UCHT1; BioLegend), anti-CD8 BV605 (clone SK1; BioLegend), anti-CD4 PE-Cy7 (clone OKT4; BioLegend), and LIVE/DEAD violet viability dye (Life Technologies).

Generalized estimating equation (GEE)

GEE was performed using "geepack" package (version 1.3.9) in R[1]. In the GEE model, family was set as "gaussian", and the correlation structure ("corstr") was set as "independence". Quasi Information Criterion (QIC) was used to compare models using "independence", "exchangeable" and "ar1" and the one with "independence" had the lowest QIC. Monoclonal antibody (Mab) use, weeks since symptom onset or first positive PCR, numbers of vaccinations before enrollment, sex, and age were adjusted for in these models. Logarithm base 10 of the neutralizing antibody levels were treated as dependent variables and other variables as independent. Coefficients for all the independent variables were then transformed to the power of 10 and was shown in this figure as fold-change compared to reference group.

Supplementary Tables

Supplementary Table 1. Categorization for immunocompromising conditions.

Non-Severe (NS)		• Autoimmune disease, receiving immunosuppressants that are not B cell/plasma cell targeted therapy within 12 months of study entry • Solid malignant tumor on treatment (excluding those who underwent resection and were considered in remission after resection) • Corticosteroid use equivalent to Prednisone >20mg daily for at least 14 consecutive days within 30 days prior to study entry • HIV infection with CD4 cell count >200 cells/mm^3
Severe	Severe- Hematological malignancy/Transplant (S-HT)	• Solid organ transplant (SOT) • Hematopoietic stem cell transplant (HSCT) • Lymphoma, leukemia • Immune-Related Adverse Event (irAE) on multiple immunosuppressants targeting different pathways
	Severe- Autoimmune and other B cell deficiency (S-A)	• Autoimmune disease receiving B cell targeted therapy within 12 months of study entry • Congenital or late onset B cell deficiency (e.g. Common Variable Immunodeficiency)

Supplementary Table 2. Diagnoses for immunocompromised participants and categorization.

ID	Diagnosis	Immunosuppressants/Treatment	Group
100	Antiphospholipid syndrome	Prednisone, eculizumab, rituximab, cyclophosphamide	S-A
101	Heart and kidney transplant	Everolimus, Prednisone 5mg daily, Tacrolimus	S-HT
107	Rheumatoid arthritis	Tocilizumab	NS
113	Minimal change disease	Rituximab within 12 months of COVID-19	S-A
126	RA	Abatacept+ Prednisone 5mg daily	NS
217	RA	Methotrexate+ Prednisone 5mg daily	NS
240	Chronic myelogenous leukemia	Dasatinib	S-HT
245	Diffuse large B-cell lymphoma	Rituximab+Polatuzumab+Prednisone, CAR-T, Chemotherapy, Tocilizumab	S-HT
388	Adenocarcinoma of pancreas	Chemotherapy and radiation	NS
449	Granulomatosis with polyangiitis	Rituximab within 12 months of COVID-19	S-A
459	Immune Related Adverse Events, Metastatic Merkel cell carcinoma	Pembrolizumab, Tacrolimus, Prednisone, Mycophenolate	S-HT
470	Multiple sclerosis	Ocrelizumab within 12 months of COVID-19	S-A
471	Marginal zone lymphoma (CR)	Obinutuzumab+CHOP	S-HT
475	Multiple sclerosis	Rituximab within 12 months of COVID-19	S-A
497	Diffuse large B-cell lymphoma (CR), Hypogammaglobulinemia	Rituximab-CHOP	S-HT
531	Sarcoidosis	Infliximab	NS
532	Granulomatosis with polyangiitis	Mycophenolate	NS
533	Diffuse large B cell lymphoma, Hypogammaglobulinemia after CAR-T	CAR-T, Tocilizumab, Pembrolizumab, Rituximab, Corticosteroid	S-HT
534	RA, Sjogren's syndrome, Hypogammaglobulinemia; cryoglobulinemia	IVIG	S-A
547	RA	Tocilizumab+Methotrexate	NS
548	RA	Rituximab within 12 months of COVID-19+ Leflunomide	S-A
549	Bechet's disease	Azathioprine	NS
550	RA	Methotrexate+ Hydroxychloroquine	NS
551	Psoriatic arthritis	Infliximab	NS
552	Seronegative spondyloarthropathy	Adalimumab+ Methotrexate	NS
557	RA, SLE	Methotrexate	NS
558	SLE	Belimumab	S-A
563	RA	Adalimumab	NS
564	Multiple myeloma	Daratumumab+ Dexamethasone	S-HT
569	SLE	Hydroxychloroquine+ Methylprednisolone daily 6mg	NS
573	Inflammatory arthritis	Adalimumab+ Hydroxychloroquine	NS

597	Giant cell arteritis, polymyalgia rheumatica	Tocilizumab+ Prednisone orally 5mg daily	NS
604	CVID	IVIG every 4 weeks	S-A
610	Ulcerative colitis	Infliximab	NS
658	RA	Tocilizumab	NS
678	RA	Tofacitinib	NS
687	SLE, RA	Hydroxychloroquine, methotrexate	NS
688	Mantle cell lymphoma	Zanubrutinib+Venetoclax; Last dose of Obinutuzumab within 12 months	S-HT
691	RA	Rituximab	S-A
708	Minimal change disease	Rituximab	S-A
716	RA	Methotrexate	NS
723	Multiple sclerosis, acquired hypogammaglobulinemia	IVIG every 4 weeks; Ocrelizumab within 12 months	S-A
725	RA	Infliximab, methotrexate, hydroxychloroquine	NS
735	Psoriatic arthritis	Adalimumab	NS
768	Ankylosing spondylitis	Secukinumab	NS
793	RA	Adalimumab, methotrexate	NS
805	Ulcerative colitis, inflammatory arthritis	Golimumab, methotrexate	NS
870	Mantle cell lymphoma	Bendamustine and rituximab within 12 months	S-HT
892	HIV infection	N/A, on antiretroviral therapy, CD4 cell count>200	NS
936	RA	Etanercept, hydroxychloroquine	NS
945	IgG4 related disease	Rituximab	S-A
946	Diffuse large B-cell lymphoma	R-CHOP	S-HT
952	Inflammatory arthritis	Adalimumab	NS
953	RA	Infliximab, methotrexate, prednisone 3mg	NS
965	Breast cancer	Trastuzumab deruxtecan within 12 months, then Olaparib	NS
982	Follicular lymphoma	Bendamustine, Obinutuzumab within 12 months	S-HT

S-HT, severe hematological oncology/Transplant; S-A, severe autoimmune disease/B-cell deficient; NS, non-severe immunocompromise; CAR-T, chimeric antigen receptor T-cell therapy; CR, complete remission; CHOP, cyclophosphamide, doxorubicin, vincristine, and prednisone; R-CHOP, Rituximab in combination with CHOP; RA, rheumatoid arthritis; SLE, systemic lupus erythematosus; CVID, common variable immunodeficiency

Supplementary Table 3. Monoclonal antibody use.

	S-HT (N=12)	S-A (N=13)	NS (N=31)	None (N=184)	Overall (N=240)
Bamlanivimab-Etesevimab	1	0	0	4	5
Casirivimab-Imdevimab	0	2[b]	2	5	9
Sotrovimab	4[a]	1	1	0	6
Bebtelovimab	3	2	2	1	8
Tixagevimab-Cilgavimab	5[c]	4	0	0	9

a, three participants received Sotrovimab after blood draws.

b, one participant received Casirivimab-Imdevimab after blood draws.

c, two participants received both Tixagevimab-Cilgavimab and Sotrovimab and one participant received

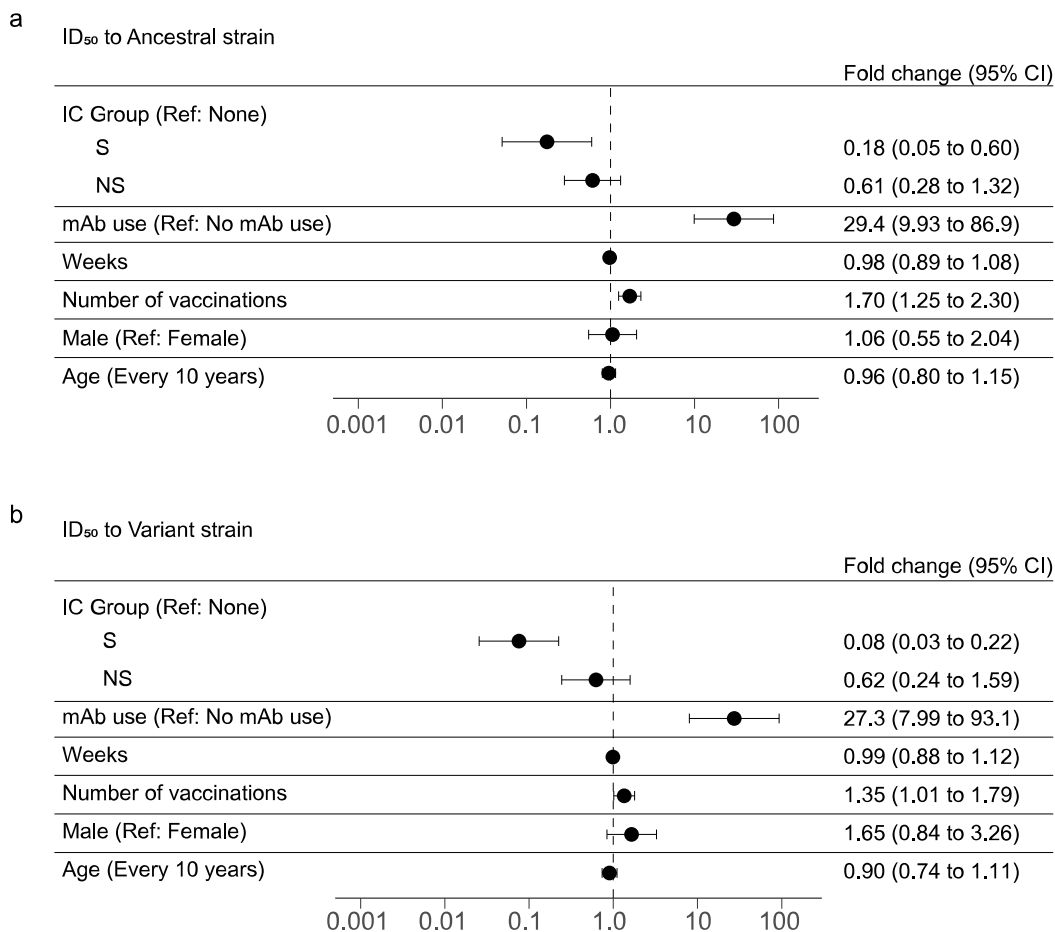both Tixagevimab-Cilgavimab and Bebtelovimab

Supplementary Figures
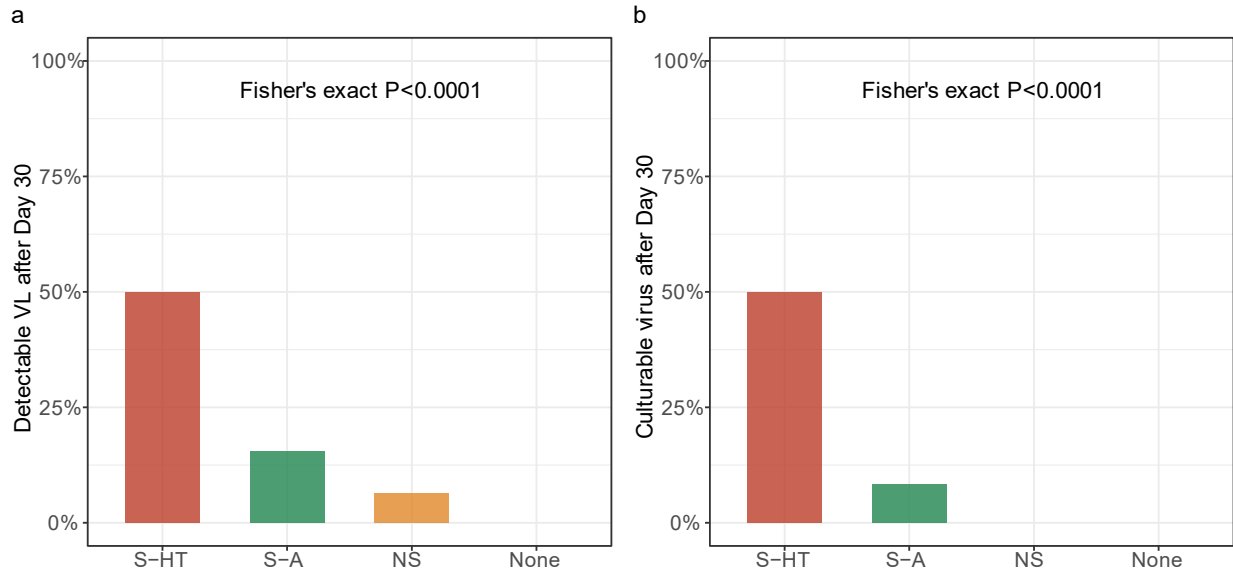
Supplementary Figure 1. Detectable SARS-CoV-2 viral RNA (a) and culturable SARS-CoV-2 virus (b) beyond 30 days after symptom onset or first positive PCR/antigen tests, supplemental to Fig. 1.

Fisher's exact test was used to calculate the P values.
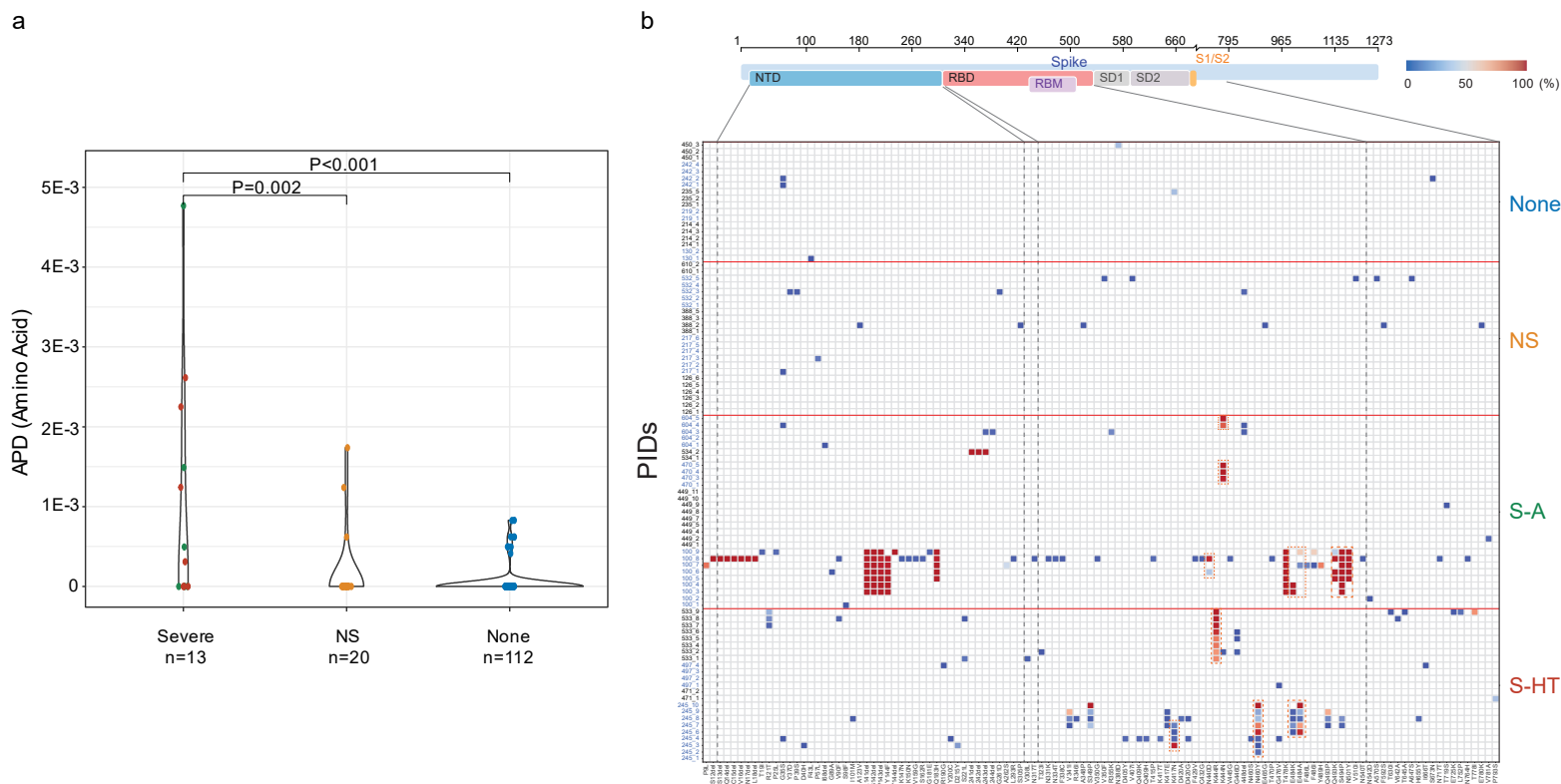
Supplementary Figure 2. SARS-CoV-2 mutations among different immunocompromised groups, supplementary to Fig. 2.

(a), SARS-CoV-2 intrahost mutations at the amino acid level among different immunocompromise groups. (b), Heat map showing distribution of Spike polymorphisms from participants receiving mAb treatment longitudinally. In the heatmap, y axis indicates participants' ID (PID) followed by sequential numbers of sample collection, while x axis shows amino acid positions in the Spike gene. Different domains of Spike are shown at the top. Colors indicate frequency of polymorphisms, with blue indicating the lowest value and red indicating the highest value in the scale. Participants in different study groups are separated by a red horizontal line. mAb resistance mutations are shown by red dotted box.

a

ID_{50} to Ancestral strain

	Fold change (95% CI)
IC Group (Ref: None)	
S	0.18 (0.05 to 0.60)
NS	0.61 (0.28 to 1.32)
mAb use (Ref: No mAb use)	29.4 (9.93 to 86.9)
Weeks	0.98 (0.89 to 1.08)
Number of vaccinations	1.70 (1.25 to 2.30)
Male (Ref: Female)	1.06 (0.55 to 2.04)
Age (Every 10 years)	0.96 (0.80 to 1.15)

0.001   0.01   0.1   1.0   10   100

b

ID_{50} to Variant strain

	Fold change (95% CI)
IC Group (Ref: None)	
S	0.08 (0.03 to 0.22)
NS	0.62 (0.24 to 1.59)
mAb use (Ref: No mAb use)	27.3 (7.99 to 93.1)
Weeks	0.99 (0.88 to 1.12)
Number of vaccinations	1.35 (1.01 to 1.79)
Male (Ref: Female)	1.65 (0.84 to 3.26)
Age (Every 10 years)	0.90 (0.74 to 1.11)

0.001   0.01   0.1   1.0   10   100

Supplementary Figure 3. Severe immunocompromise is associated with lower neutralizing antibody levels, supplemental to Fig. 3.

Generalized estimation equation to account for longitudinal repeated measurements was used to estimate the association between immunocompromise groups and neutralizing antibody levels against ancestral SARS-CoV-2 Spike protein (a) and variant-specific Spike protein (b). Monoclonal antibody (mAb) use, weeks since symptom onset or first positive PCR/antigen, numbers of vaccinations before enrollment, sex, and age were adjusted for in these models.
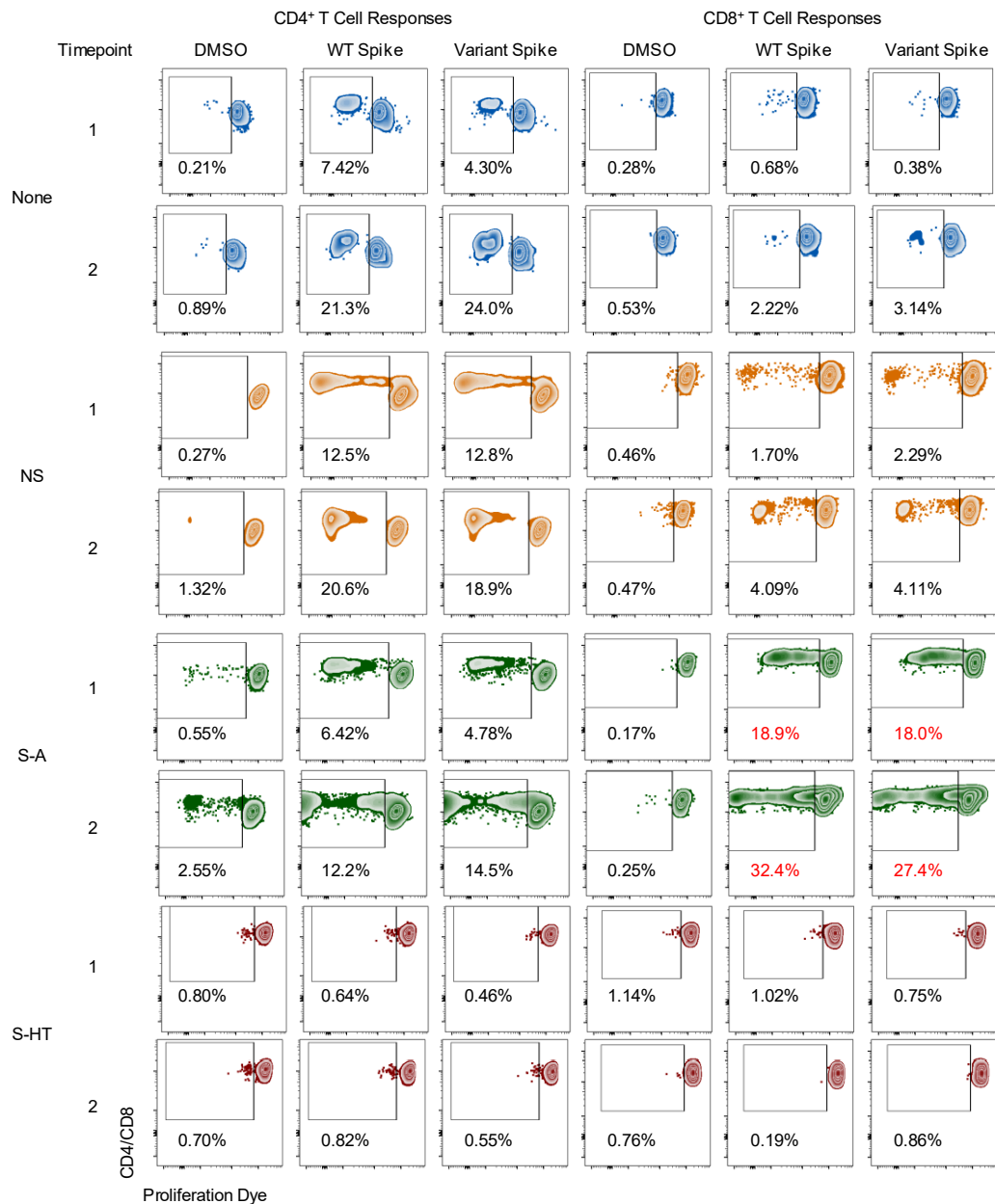
Supplementary Figure 4. Representative T cell proliferation assay gating scheme,
supplementary to Fig. 4.

CD4+ and CD8+ T cell proliferation results from representative participants in each
immunocompromise group are shown. Non-immunocompromised group, ID=261 (Omicron,
BA.1); Non-severe group (NS), ID= 768 (Omicron, BF.5); Severe-autoimmune/B-cell deficient
(S-A), ID=534 (Omicron, BA.2); Severe- hematological malignancy/transplant (S-HT), ID= 245
(Delta, B.1.617.2).
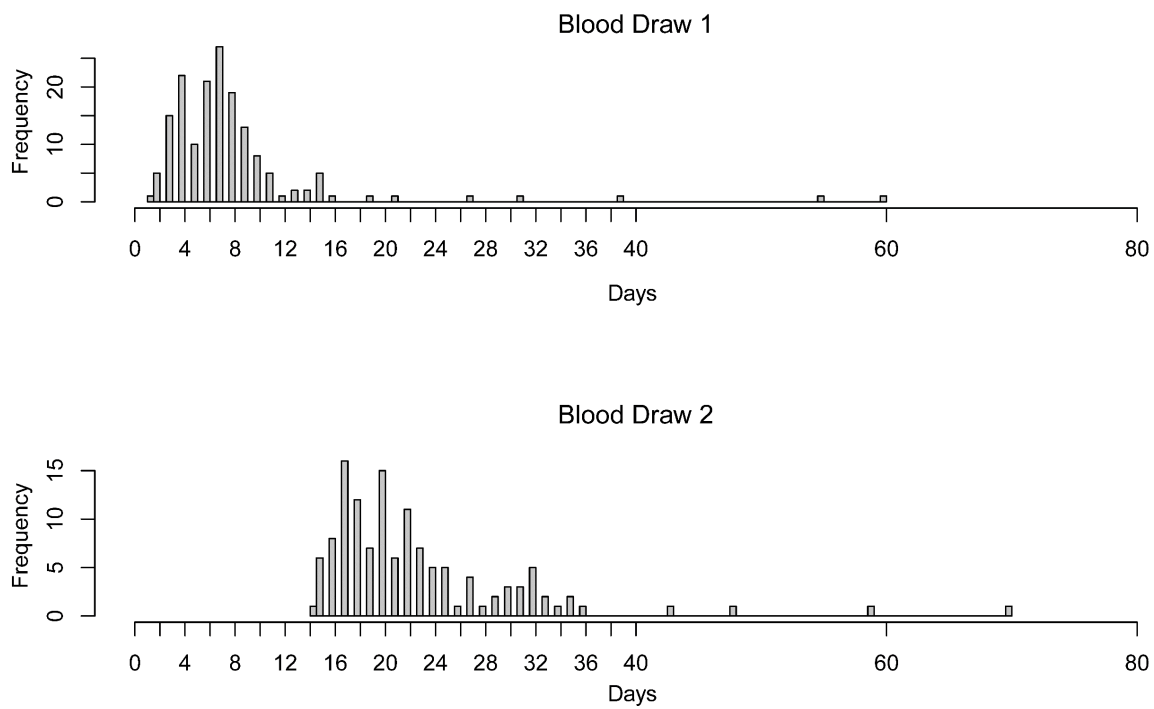
Supplementary Figure 5. Distribution of duration between symptom onset or first positive PCR and blood draws.

References

1. Højsgaard, S., Halekoh, U. & Yan, J. The R Package geepack for Generalized
   Estimating Equations. *Journal of Statistical Software* **15**, 1 - 11 (2005).